

AD-A084 436

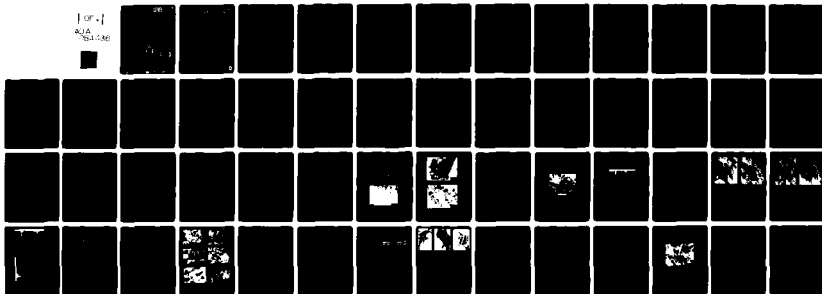
CINCINNATI UNIV OHIO DEPT OF MATERIALS SCIENCE AND --ETC F/8 11/6
MICROSTRUCTURAL EFFECTS AND FATIGUE LIFE PREDICTIONS OF NOTCHED--ETC(U)
APR 80 S D ANTOLOVICH AFOSR-76-2952

UNCLASSIFIED

AFOSR -TR-80-0341

NL

[of-]
AIA
784-08



END
DATE
FILMED
6-80
DTIC

AFOSR-TR- 80 - 0341

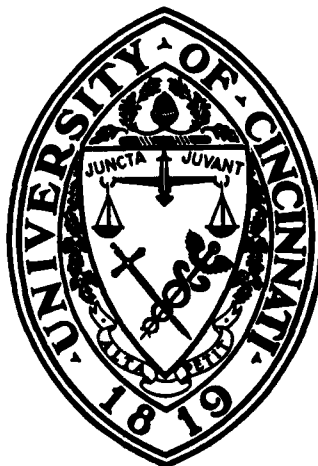
LEVEL

III
No 552 5 86

12

UNIVERSITY OF CINCINNATI

ADA 084436



DTIC
ELECTE
MAY 20 1980
S **D**
D

Department of
Materials Science and Metallurgical Engineering

University of Cincinnati
Cincinnati, Ohio 45221

Approved for public release;
distribution unlimited.

DDC FILE COPY

80 5 14 0 80

Accession For	
NTIS GRA&I	<input checked="" type="checkbox"/>
DDC TAB	<input type="checkbox"/>
Unannounced	<input type="checkbox"/>
Justification	<input type="checkbox"/>
By _____	
Distribution/	
Availability Codes	
Dist.	Avail and/or special
A	

LEVEL III

D

6 Microstructural Effects and Fatigue Life Predictions of Notched and Un-notched Ni Base Superalloys at Elevated Temperatures.

15 Final Report AFOSR-76-2952

Jan. 1, 1976 - Dec. 31, 1979

14 Stephen D. Antolovich

11 April 1979
12 54

9 Final Report 1 Jan 76 - 31 Dec 79

16 2306

17 A1

18 AFOSR

19 TR-84-0304

AFOSR
A. D. BLOSS
Technical Information Officer

DTIC ELECTE
MAY 20 1980
S D D

405382

Unclassified

SECURITY CLASSIFICATION OF THIS PAGE (When Data Entered)

REPORT DOCUMENTATION PAGE		READ INSTRUCTIONS BEFORE COMPLETING FORM
1. REPORT NUMBER AFOSR-TR- 80 - 0341	2. GOVT ACCESSION NO. <i>AD-A084436</i>	3. RECIPIENT'S CATALOG NUMBER
4. TITLE (and Subtitle) Microstructural Effects and Fatigue Life Predictions of Notched and Un-notched Ni Base Superalloys at Elevated Temperatures		5. TYPE OF REPORT & PERIOD COVERED Final Jan. 1, 1976 - Dec. 31, 1979
7. AUTHOR(s) Dr. Stephen D. Antolovich		6. PERFORMING ORG. REPORT NUMBER
9. PERFORMING ORGANIZATION NAME AND ADDRESS University of Cincinnati Dept. of Materials Science and Metallurgical Engineering		8. CONTRACT OR GRANT NUMBER(s) AFOSR-76-2952
11. CONTROLLING OFFICE NAME AND ADDRESS AF Office of Scientific Research / <i>NE</i> Bolling Airforce Base, Building 410 Washington, D.C. 20332		10. PROGRAM ELEMENT, PROJECT, TASK AREA & WORK UNIT NUMBERS 61102F 2306/A1
14. MONITORING AGENCY NAME & ADDRESS (if different from Controlling Office)		12. REPORT DATE April 1980
		13. NUMBER OF PAGES 51
		15. SECURITY CLASS. (of this report) Unclassified
		15a. DECLASSIFICATION/DOWNGRADING SCHEDULE
16. DISTRIBUTION STATEMENT (of this Report) Approved for public release; distribution unlimited.		
17. DISTRIBUTION STATEMENT (of the abstract entered in Block 20, if different from Report)		
18. SUPPLEMENTARY NOTES		
19. KEY WORDS (Continue on reverse side if necessary and identify by block number) Ni base superalloys, René 80, René 77, high temperature low cycle fatigue, optical microscopy, scanning electron microscopy, transmission electron microscopy, notch low cycle fatigue, creep/fatigue interactions. <i>(Low cycle fatigue)</i>		
20. ABSTRACT (Continue on reverse side if necessary and identify by block number) → The LCF behavior of Ni base superalloys was studied both for smooth and notched test bars. The primary research material was René 80 which finds application in turbine blades used in the temperature range of 650-982°C (1200-1800°F). The smooth bar LCF behavior was studied in the as-heat treated condition and also after exposure for 100h at 982°C, either under →		

a stress of 97 MPa (14 ksi) or OMPa. Test conditions included continuous cycling at different strain rates as well as 90 second hold periods at either maximum or minimum strain. The primary test temperatures were 871°C (1600°F) and 982°C (1800°F). It was found that prior exposure greatly reduces the fatigue life, especially when stress exposed specimens are tested at high strain rates. Since these experiments tend to duplicate actual engine conditions, use of data obtained using as-heat treated specimens may be very non-conservative to predict lives of actual components. When exposed specimens were re-machined prior to testing, the original life was restored and to a small degree improved. These experiments showed that the primary damage mechanism was surface related. This conclusion was substantiated by both optical and electron microscopy.

For the as-heat treated specimens, the life generally increased with decreasing test frequency or with hold time, contrary to what is observed for many other systems and predicted by other theories. It was again observed that the principal damage mechanism was oxidation of surface connected grain boundaries.

The test results, including results for exposed specimens ~~all~~ correlated very well with a model for LCF ~~that~~ was developed and which is based on the concept that cracks initiate at a critical combination of oxide depth (or oxygen penetration) and stress.

The notch LCF problem was also studied. A computer model for calculating local stresses and strains was developed, and the concept of a critical energy dissipated in a process zone was used as a failure criterion. The model also incorporated the observation that the principal form of damage was an environmental interaction. Comparison of experiment and theory was excellent at high temperature where oxidation is in fact the prevalent damage mode.

In addition to the René 80 studies, some initial smooth bar LCF studies were carried out using René 77, which has a precipitate structure similar to René 80. These studies also showed that the most severe form of damage was oxidation and that plastic deformation acts as a catalyst for rapid precipitate coarsening.

TABLE OF CONTENTS

I.	INTRODUCTION	1
II.	MATERIALS, HEAT TREATMENT AND SPECIMENS	2
	A. Materials and Heat Treatments	2
	B. Specimens	2
III.	SMOOTH BAR LCF STUDIES	3
	A. René 77	3
	B. René 80	4
	1. Effect of Prior Exposure	4
	2. Effect of Hold Time and Strain Rate	5
	3. A Model for High Temperature LCF	6
IV.	NOTCH LCF STUDIES	9
	A. Introduction	9
	B. Finite Element Method (FEM) Analyses	10
	C. Notched LCF Test Results	12
	D. Correlation of Model Prediction and Test Results	12
	E. Application to Mechanistic Model to Notch LCF Life Prediction	13
V.	SUMMARY AND CONCLUSIONS	16
	A. René 77	16
	B. Smooth Bar LCF of As-Heat Treated René 80	17
	C. Smooth Bar LCF of Exposed René 80	18
	D. Notch LCF of As-Heat Treated René 80	19
VI.	PERSONNEL	20
VII.	PUBLICATIONS AND PRESENTATIONS ON AFOSR 76-2952	21
VIII.	INTERACTIONS WITH A. F. PERSONNEL AND OTHER AFOSR SPONSORED P.I.'s	23
	REFERENCES	

I. INTRODUCTION

Although several methodologies exist for the prediction of fatigue life at elevated temperature⁽¹⁻⁴⁾, none of them are based on a well-defined damage mechanism. While each of these may work in certain well-defined situations, they are not generally applicable nor is there any guidance for the conditions and materials for which they might be expected to apply. In view of the complexity of possible damage processes (e.g. dislocation debris, grain boundary void formation, oxidation, phase changes) it is not probable for a given formulation of fatigue life to be universally applicable. Instead, it would appear that fatigue life formulations must be defined in terms of classes of materials and temperature ranges.

In this study René 80, a cast Ni base superalloy used for turbine blades was the primary material studied. In addition, René 77 (or Udimet 700) was investigated in the initial phases of the project. The goal of the project was to study mechanisms of damage in these important materials and based on mechanisms that were identified, to develop life prediction techniques for both smooth and notched components. The details of the project are discussed in subsequent sections.

II. MATERIALS, HEAT TREATMENT AND SPECIMENS

A. Materials and Heat Treatments

The René 80 was purchased from MISCO in the form of cast to shape test bars. The composition and heat treatment are shown in Table I. The composition lies well within the specification for René 80. The heat treatment is close to the commercial treatment except that final ageing was carried out at 1400°F to maximize the strength. The microstructure is shown in Figs. 1 and 2. The grains are large, irregular and decorated with carbides while the precipitate structure consists of large cubes and small spheres.

The René 77 composition and heat-treatment are shown in Table II. The microstructure is similar to René 80 except that the René 77 was in the wrought condition and hence had a much smaller grain size with more regular grain boundaries.

B. Specimens

In all cases standard tensile and LCF specimens were used. For René 80, longitudinal LCF specimens were employed while hour glass LCF specimens were used for the René 77. All specimens were finish machined after heat treatment by low stress grinding to minimize the surface effect.

III. SMOOTH BAR LCF STUDIES

A. René 77

The René 77 test results are represented in terms of a Coffin-Manson plot in Fig. 3. The testing was carried out at 1700°F (927°C) at both high and low frequencies. There was no effect of test frequency. Contrary to what might be expected on the basis of several theories of creep/fatigue interactions no degradation in life occurred.

Damage mechanisms were studied by scanning electron microscopy (SEM) and by transmission electron microscopy (TEM). Typical results are seen in Figs. 4 and 5. It can be seen that the effect of LCF was to cause rapid coarsening of the precipitate structure as seen in Fig. 4. Furthermore, there was a buildup of interfacial dislocations on the precipitate interface. It was demonstrated that these dislocations were near-edge and took up the misfit between matrix and precipitate. On this basis it can be concluded that the dislocation "debris" does not represent any form of damage. Furthermore, there was no evidence of grain boundary sliding so this was also ruled out as a damage process. The major form of damage turned out to be oxidation of grain boundaries and twins as can be seen in Fig. 5. The degrading effect of environment was demonstrated by oxidizing a specimen for 7 hours at 927°C and then re-heat treating. This specimen was tested at room temperature and compared to another specimen that was not oxidized. It can be seen that there was a life reduction of a factor of 2. This result is a lower bound of the oxidation effect

since at high temperatures the process takes place under stress and can be greatly accelerated. The details of this study have been discussed at length in a paper submitted for publication⁽⁵⁾.

B. René 80

The LCF properties of René 80 were studied at 1400°F (760°C), 1600°F (871°C) and 1800°F (982°C) with emphasis on testing at 1600 and 1800°F. The test matrix was much more extensive than for René 77, and incorporated hold time tests at both maximum and minimum strain, continuous cycling tests at different strain rates and continuous cycling of specimens that had been exposed for 100h (either stress free or at 1/3 the yield) prior to testing. The results of this study were internally very consistent, but at variance with many commonly accepted ideas for high temperature LCF. The results obtained for this phase of the project are discussed in subsequent sections.

1. Effect of Prior Exposure

Since the engine conditions are such that blades are under load for long periods of time under stress it was deemed important from a practical point of view to compare specimens that had been exposed prior to testing to results obtained for as-heated specimens. The exposure was done in two ways. In the first case specimens were placed in a furnace for 100 hrs at 1800°F (982°C) and subsequently tested at 1600°F (871°C). This was done since numerous studies in the literature on the stability of Ni base superalloys were done by simple thermal exposure under stress free conditions. The higher exposure temperature was used since

turbine blades actually are used at this temperature and to accelerate any processes that would occur at lower temperatures. In the second case specimens were exposed at 1800°F (982°C) for 100 hrs at a stress of 14 ksi (97 MPa) prior to LCF testing. Tests were carried out at either 20 cpm or 2 cpm and the results are shown in Fig. 6. It can be seen that the effect of simple thermal exposure was to somewhat decrease the fatigue life while stress exposure caused a dramatic decrease in the fatigue life. The decrease was most pronounced when the cycle rate was highest contrary to some theoretical predictions. The life was restored when stress exposed specimens were re-machined prior to testing. These results show that the damage was surface-related and that any changes taking place internally were minimally beneficial. The internal structure is shown in Fig. 7. The small precipitates have dissolved and the large ones have grown, becoming more irregular and acquiring an array of interfacial dislocations. The surface structure is seen in Fig. 8. Cracks are seen to initiate at surface-connected grain boundaries where oxidation or oxygen penetration is severe. These studies were reported in detail in a recently published paper⁽⁶⁾.

2. Effect of Hold Time and Strain Rate

The effect of both hold time and strain rate was studied at 1600°F (871°C) and 1800°F (982°C) and the results are shown in Figs. 9 and 10. It is noteworthy that the LCF life *increases* when the strain rate is decreased or a hold time is imposed. This again is counter to what is observed in many other systems and to

the prediction of many theories. The increase in life appears to be most pronounced for the lower strain ranges where the lives are in the range of engineering interest.

The damage mechanisms were studied both by optical and electron microscopy. The internal structural changes are summarized in Fig. 11. It can be seen that as either the temperature or cycle period increases, the small precipitates dissolve and the large precipitates tend to agglomerate on {100} planes and acquire interfacial dislocations which are of edge character. Such changes, as already mentioned, do not constitute damage. Again, the major form of damage was surface oxidation similar to that seen in Fig. 8. These observations are incorporated into a model for LCF in the following section.

3. A Model for High Temperature LCF

The results cited in previous sections lead to the hypothesis that deformation related damage such as dislocation debris and grain boundary sliding are of minimal importance in determining the LCF life at elevated temperatures. In fact, the *internal* changes that were observed tend to improve the life. The major damage was surface-related, probably taking the form of grain boundary oxidation or oxide penetration. As the metal is cycled, an embrittled region forms and after attaining a critical size the embrittled region fractures at the maximum stress in a cycle. Clearly, the maximum stress depends on the metallurgical microstructure (grain size, precipitate size and character) and the

deformation mode. In a given system, fracture of the embrittled region will depend on the size of the affected zone and the stress. The stress, in a strain-controlled test will depend on any structural changes that occur. Thus, if a material undergoes significant coarsening, the flow stress will be reduced and a larger environmentally affected region could be tolerated before crack initiation. These ideas and their experimental foundations have been developed fully in two recent publications^(7,8). The main result is that the fatigue life can be correlated to the following equation:

$$N_i = \frac{C_1}{D \left[t_e + \left(\frac{1}{v} + t_h \right) \right] \cdot (\sigma_i^{\max})^8} \quad \dots(1)$$

- where N_i = cycles to initiation
 C_1 = ductility-related constant
 D = diffusion constant
 t_e = exposure time prior to test
 v = cycle frequency (excluding any hold time)
 t_h = hold time
 σ_i^{\max} = maximum stress in a hysteresis loop at the point of crack initiation.

The above equation is based on the assumption that parabolic oxidation kinetics are obeyed which was verified by metallographic observations. The high degree of correlation of the data to eq. 1 is shown in Figs. 12 and 13.

Based on the good correlation of the data with the theory we may conclude that the reason for the increase in life with lower

frequency or hold time is due to the fact that the structural coarsening leads to a reduced stress. This meant that the damage zone could be larger before fracture and that more cycles could be accumulated.

For illustrative purposes, eq. 1 can be applied to a material that is stable and in which there is no pre-exposure. The result is

$$N_i = C_2 (v/1 + vt_n) \exp Q/RT \cdot \Delta\epsilon_p^{-8n'} \quad \dots(2)$$

where C_2 = constant

Q = activation energy for oxidation

R = gas constant

T = temperature.

$\Delta\epsilon_p$ = plastic strain range

n' = cyclic strain hardening exponent.

It is interesting that eq. 2 has the same form as Coffin's frequency modified fatigue life with explicit evaluation of frequency and temperature dependence. For stable materials tested in fully reversed fatigue eq. 2 predicts decreases in life for low frequency, long hold time and high temperature. Such behavior is, in fact, frequently observed. Moreover, values of n' are frequently in the range of 0.15 to 0.20 which according to eq. 2 implies Coffin-Manson exponents on the order of 0.6 to 0.8. Again such values are commonly observed.

Finally, based on the development of the above model, it may be concluded that agreement of experimental data with a Coffin-Manson representation does not necessarily imply damage accumulation by deformation debris as has been frequently assumed.

IV. NOTCH LCF STUDIES.

A. Introduction

An analytical and experimental investigation of the low cycle fatigue (LCF) behavior of circumferentially notched round bars of René 80 in the temperature range 760°C - 982°C was completed. The specific objective of this work was to develop a mechanistically based design tool for LCF life prediction for notched components manufactured from Ni-base superalloys. To achieve this goal, detailed finite element method (FEM) elastic-plastic model analyses were combined with light optical, scanning (SEM) and transmission (TEM) microscopy to mathematically and mechanistically characterize the problem.

A method based on strain-energy density and the concept of a local, active, notch root volume was developed. The method uses a post-processor calculation, ordering, and summing routine that supplements a FEM model solution and hence is very suited to current industry approaches to life prediction. Certain material dependent considerations complicate the determination of the active zone size, however.

In addition to the FEM approach, the mechanistic model developed earlier for the LCF behavior of smooth bars was studied in relation to its adaptability to the notched problem. Consistent with the objective of this effort it was found that analytic FEM results can be combined with the mechanistic model to arrive at a rational approach to notch life assessment.

The analytic studies were supported by cyclic fatigue tests of notched bars. Test results were compared to the analytical predictions at 760°C and 982°C. In general, results at 982°C were well predicted within the limits of the models considered, while at 760°C a marked increase in data scatter was observed, making meaningful comparisons difficult.

The objective of this phase of the project was achieved in essence. The FEM energy method and the mechanistic model have limitations that depend on microstructural features of René 80 at the appropriate temperatures. This, however, is an improvement over purely empirical approaches where limitations and hence, reliability are often unknown and more importantly not understood.

B. Finite Element Method (FEM) Analyses

FEM models using the computer codes described in Ref. 9 were created for the notched specimen shown in Fig. 14. Two notch geometries were considered with nominal stress concentration factors (K_T) of 3.0 and 2.0 as determined from Ref. 10. Elastic solutions revealed FEM calculated K_T 's of 3.49 and 2.22 consistent with other published FEM results⁽¹¹⁾. Elastic-plastic solutions were obtained for numerous load conditions at 760°C, 871°C, and 982°C. The model is capable of addressing variations in material response caused by different strain rates through the inclusion of appropriate cyclic stress-strain curves. Analyses were completed using stress-strain curves obtained from LCF tests conducted on smooth bars at strain rates of 50%/min. and 0.5%/min.

The output from these various models provides amplitudes and distributions of cyclically varying axial, tangential, radial, and effective stress, elastic strains, and plastic strains at any point in the model.

Following the work of Ostergren⁽⁴⁾ and Leis⁽¹²⁾ it was anticipated that a strain energy approach to LCF life prediction was appropriate since it incorporates both stress and strain as potential independent variables. Further, since this energy can be conveniently averaged over a volume and the concept of an active or critical volume of material involved in the fatigue process has been considered^(13,14), a method of calculating the average notch root plastic strain energy density was developed. Using a post-processor to address the tape-stored FEM results, the volume and energy contained in each of the 612 elements is determined. The elements are ordered as a function of energy density and the results tabulated in a cumulative format. Figure 14 ($K_T = 3.49$, 982°C , $50\%/min$) illustrates typical results. For a suitably chosen critical volume (maximum volume is the notch root plastic zone size) the cumulative energy or average energy (energy density) can be obtained from this figure.

From a plot of hysteresis loop energy versus fatigue life for smooth bar specimens (obtained from smooth bar results), entered with the energy density obtained for the notched analysis the predicted notch LCF life is obtained.

C. Notched LCF Test Results

LCF tests were completed on René 80 circumferentially notched specimens machined from cast to size bars. Test frequencies were established and controlled so as to obtain a calculated local notch axial strain rate of 50%/min or 0.5%/min for continuous cycled tests. Tests with 50%/min or 0.5%/min ramp frequencies with a 90 sec. tensile hold period were also run. Specimens with $K_T = 3.49$ and $K_T = 2.22$ were tested at 982°C while 760°C testing was limited to $K_T = 3.49$. The results of these tests are shown in Figs. 15-18. From the figures, it is apparent that at 982°C as frequency is decreased life decreases. Life is generally further decreased with hold time except that for the lower K_T at high nominal stresses the hold time and continuous results are similar. This is expected due to the short lifetimes and the lack of sufficient time for additional environmental degradation. At 760°C considerable data scatter was observed as seen in Fig. 18. This is discussed further in the following section.

D. Correlation of Model Prediction and Test Results

Figure 15 shows the agreement obtained between predictions (based on a critical volume assumed equal to the plastic zone size, $K_T = 3.49$, local notch root strain rate equal 50%/min) and test results at 760°C and 982°C.

Also shown in the figure are optical micrographs of typical notch root failure sites. At 982°C the failure mechanism is dominated by surface degradation due to oxidation especially at

grain boundaries at the notch root. TEM micrographs of smooth bars have shown few dislocations in the matrix with a coarsened γ' structure and interfacial dislocations. The dominance of an environmental (oxidation) mechanism leading to crack formation prompted the use of the axial stress and strain components (consistent with fracture mechanics concepts) in computing energy density. This results in excellent correlation at 982°C.

At 760°C the grain boundary oxidation remains an important consideration, but the deformation is restricted to well-defined bands and the accumulation of deformation debris is more important (deformation bands of dislocations) at this temperature. Deformation bands can be seen quite clearly in Fig. 19. The combination of slip bands in the matrix and grain boundary oxidation appears to have potential for a severe notch life penalty. In Fig. 15, several of the test results are reasonably well predicted by the method while several others have much reduced life. This suggests a critical notch root volume smaller than the plastic zone is operational for these tests.

E. Application of Mechanistic Model to Notch LCF Life Prediction

The mechanistic model developed previously can be applied to notch bar life predictions. The mechanistic model was developed by assuming a uniform stress in the bar and was based on an observation that oxidation spike depth λ_i followed the relation:

$$\sigma_i^{\max} \cdot \lambda_i^{1/4} = C_0 \quad \dots(3)$$

For notched components the stress is not uniform but follows a

distribution that may be approximated by a polynomial:

$$\sigma_i(x)^{\max} = \sum_{K=0}^n A_K X^K \quad \dots(4)$$

If the average stress over the spike length is assumed to follow the same relation (3) then

$$\frac{\int_0^{\ell_i} \sigma_i(x)^{\max} dx}{\ell_i} \cdot \ell_i^{1/4} = C_0 \quad \dots(5)$$

or substituting 4 into 5 and integrating:

$$\sum_{K=0}^n \frac{A_K \ell_i^{\frac{4k+1}{4}}}{(k+1)} = C_0 \quad \dots(6)$$

and Equation (1) becomes:

$$\sum_{K=0}^n \frac{[A_K D^{(1/\nu + t_n)} N_i]}{(k+1)} \frac{4k+1}{8} = C_0 \quad \dots(7)$$

For an assumed constant distribution, eq. (7) reduces to eq. (1). Figure 20 shows the results of applying the eq. 7 model with an assumed uniform maximum stress equal to the notch root axial stress. The continuous cycled results correlate well as was the case for smooth bar LCF. The 90 sec. holdtime results fall on a different curve. However, this is due not only to the variable stress field away from the notch, but also to the relaxation of local stresses during the holdtime. When a holdtime cycle is simulated in the FEM model, the local stress and strain history in Fig. 21 is predicted. If the relaxed local stress is

used in the model the agreement with the continuous cycle results is much improved (Fig. 20). The full details of the polynomial stress modifier and additional relaxations during subsequent cycles have yet to be studied. The present results are however, encouraging.

V. SUMMARY AND CONCLUSIONS

The major conclusion that can be drawn from this work is that LCF damage at elevated temperatures is primarily in the form of oxidation or oxide penetration along surface connected boundaries. In addition, plastic deformation acts as a catalyst for precipitate coarsening by providing easy diffusion paths along dislocations. The life is determined by the stress associated with the coarsened structure and the depth of oxidation and on this basis a theory can be developed for life prediction that incorporates frequency, hold time, mean stress and cyclic stress-strain properties. Conclusions for various specific phases of the project are given below.

A. René 77

1. The high temperature LCF properties of René 77 can be represented by a Coffin-Manson plot. This plot shows a higher fatigue ductility than is observed in a short term tensile test. The increased ductility is associated with a coarsening of the γ' structure. Furthermore, there was no apparent frequency dependence of the results in the regime studied.

2. Two distinct cracking processes were observed: grain boundary initiation associated with heavy environmental damage and transgranular/intergranular crack propagation. In no instance was it possible to correlate the initiation or propagation characteristics to the test frequency in the range studied.

3. The stable dislocation structure consisted of arrays of edge dislocations on precipitate particles. The equilibrium dislocation density was established very early in the fatigue life.

4. The γ' particles were stable with respect to thermal exposure. However, with plastic deformation, the precipitate particles coarsened very rapidly. The large precipitates tended to agglomerate and become very irregular in shape.

5. The effect of the environment was shown to be the major mechanism of damage accumulation.

B. Smooth Bar LCF of As-Heat Treated René 80

1. The fatigue life of as-heat treated René 80 at both 871°C and 982°C increases with decreased frequency and imposition of a 90 second hold time. Such behavior is at variance with the concept of a negative creep/fatigue interaction.

2. The γ' precipitates in René 80 coarsened and developed interfacial arrays of edge dislocations with very few dislocations in the matrix. Such changes do not constitute damage in any fundamental sense.

3. Cracks initiated at oxide spikes in surface connected grain boundaries. Only in the case of hold time specimens rapidly loaded to maximum strain was any internal void formation seen. Even in these cases there were also surface initiation sites.

4. The metallographic observations were used to develop a correlation between maximum stress and depth of oxidation at the

time of crack initiation. All data was well-represented by this correlation.

5. This correlation was used to develop an expression for the crack initiation life. The expression has the form of the Coffin-Manson law for a given set of experimental conditions. In addition to cyclic stress/strain parameters, frequency, hold time, and temperature are explicitly incorporated.

C. Smooth Bar LCF of Exposed René 80

1. The effect of prior exposure was to reduce the fatigue life, the reduction being largest for stress exposed specimens tested at high rates.

2. Remachining of exposed specimens had the effect of restoring the fatigue life. Failure was related to a boundary embrittlement phenomenon in the near-surface region and under the experimental conditions employed in this phase of the study, classical ideas of life degradation by creep/fatigue interactions are not applicable.

3. The slip mode was generally constant for all microstructures and frequencies studied. The dislocations were arranged in approximately hexagonal networks of near-edge orientation on the large γ' precipitates and were geometrically similar to those observed in creep specimens, indicating that a significant creep component was present during testing. The similarity of slip mode for all conditions indicates that differences in life

cannot be attributed to basic differences in the plastic deformation process.

4. Plastic deformation during LCF is generally easier in the coarsened structures as evidenced by the lower stress range for equivalent total strain ranges when compared to conventionally treated material.

5. All LCF test results for the exposed specimens correlated very well to the theory previously developed for as-heat treated specimens provided that exposure time was included in the formula.

D. Notch LCF of As-Heat Treated René 80

1. Based on test results at 982°C, as the local notch strain rate decreases life decreases. This decrease continues when 90 sec. tensile hold periods are introduced.

2. The FEM method of energy density determination and life prediction showed excellent correlation with test data for $K_T = 3.49$ at 982°C. The correlation was less good at 760°C and for $K_T = 2.22$ at 982°C. The primary limitation of the approach is difficulty in establishing an active notch root volume other than the plastic zone size.

3. The mechanistic model cited previously can probably be adapted to notch life predictions by recognizing local stress distribution and calculating the local notch relaxation occurring during hold time.

VI. PERSONNEL

All research personnel associated with this project are listed in Table III.

VII. PUBLICATIONS AND PRESENTATIONS ON AFOSR 76-2952

1. Metallurgical Aspects of High Temperature Fatigue. Fatigue of Materials and Structures, Ch. 16. Edited by Malione, Paris, France, 1980. Invited paper presented at International Conference on Fatigue, Sherbrooke, Canada 1978.
2. High Temperature Fatigue of René 80. With P. Domas. Edited by Malione. Book to appear in summer of 1980.
3. Low Cycle Fatigue of René 80 as Affected by Prior Exposure. Met. Trans., 10A, 1979, p. 1859. With P. Domas and J. L. Strudel.
4. A Mechanistically Based Model for High Temperature LCF of Ni Base Superalloys. Paper in press in the Proceedings of the 4th International Conference on Superalloys. With R. Baur and S. Liu. To be presented Sept. 1980.
5. Low Cycle Fatigue Behavior of René 80 at Elevated Temperature. Paper submitted for publication. With S. Liu and R. Baur.
6. Low Cycle Fatigue of René 77 at Elevated Temperature. Paper submitted for publication. With E. Rosa and A. Pineau.
7. The Effect of Microstructure and Environment on High Temperature LCF of Ni Base Alloys. Invited paper to be presented to the 27th AMMRC Conference Fatigue-Environment and Temperature Effects, July 1980. Written version of paper to be included in conference proceedings.
8. Environmental Effects in LCF at Elevated Temperature. Invited paper to be presented to the International Symposium on Low Cycle Fatigue, Firminy, France, Sept. 1980. Conference proceedings to be published by ASTM.
9. An Integrated Energy Density Approach to Notch LCF Prediction. Paper to be prepared with Paul Domas after completion of his Ph.D. dissertation in Aug. 1980.
10. A Mechanistically Based Model for High Temperature Notch LCF of Ni Base Superalloys. Paper to be prepared with P. Domas.

In addition to the above papers, there have been a number of presentations to professional societies. They are listed below.

11. Low Cycle Fatigue at Elevated Temperature: Theory and Practise. Invited keynote address to the French Metallurgical Society, Oct. 1979.

12. Dislocation Substructure and Precipitate Morphology of René 80 in LCF at 1400, 1600 and 1800°F. Presented at the Fall AIME Meeting, Milwaukee 1979. With S. Liu.
13. A Mechanistically Based Model for LCF of Ni Base Superalloys. With S. Liu. Ibid.
14. High Temperature LCF of René 77. Presented at Fall AIME Meeting, St. Louis 1978. With E. Rosa.

VIII. INTERACTIONS WITH A.F. PERSONNEL AND OTHER AFOSR
SPONSORED P.I.'s.

The author has maintained close contact with W. Reimann and T. Nicholas of the AFML and with R. Pelloux of MIT. In addition, there have been useful exchanges with R. Raj of Cornell and with Julia Weertman of Northwestern.

REFERENCES

1. L. F. Coffin: Proc. 2nd International Conf. on Mech. Behavior of Materials, Boston 1976, p. 866.
2. S. S. Manson: ASTM STP 520, 1973, p. 744.
3. S. Majumdar and P. S. Maiya: Proc. ASME-MPC Symposium on Creep-Fatigue Interaction, MPC-3. ASME, N.Y., 1976, p. 323.
4. W. J. Ostergren: "A Damage Function and Associated Failure Equations for Predicting Hold Time and Frequency Effects in Elevated Temperature, Low Cycle Fatigue", Journal of Testing and Evaluation, Vol. 4, no. 5, Sept. 1976, pp. 327-339.
5. E. Rosa, Stephen D. Antolovich and A. Pineau: "Low Cycle Fatigue of René 77 at Elevated Temperature. Paper submitted for publication.
6. Stephen D. Antolovich, P. Domas and J. L. Strudel: "Low Cycle Fatigue of René 80 as Affected by Prior Exposure". Met. Trans., 10A, 1979, p. 1859.
7. Stephen D. Antolovich, R. Baur and S. Liu: "A Mechanistically Based Model for High Temperature LCF of Ni Base Superalloys". To be presented at 4th International Conference on Superalloys, Seven Springs, PA., Sept. 1980, Paper in press.
8. Stephen D. Antolovich, S. Liu and R. Baur: "LCF Behavior of René 80 at Elevated Temperatures", Paper submitted for publication.
9. R. L. McKnight and L. H. Sobel: "Finite Element Cyclic Thermoplasticity Analysis by the Method of Subvolumes", Computers and Structures, Vol. 7, no. 2, April 1977, pp. 189-196.
10. H. N. Neuber: "Theory of Notch Stresses", J. W. Edwards, Ann Arbor, MI., 1946.
11. S. Taira, R. Ohtani, and T. Ito: "Creep Stress and Strain Analysis of Notched Plates and Bars by Means of the Finite Element Method".
12. B. N. Leis: "Fatigue Life Prediction of Complex Structures", Trans. of ASME, Paper no. 77-DE-46, Feb. 1977.
13. J. M. Krafft: "Correlation of Plane Strain Crack Toughness with Strain Hardening Characteristics of a Low, Medium and High Strength Steel", App. Mat. Res., Vol. 3, No. 2, 1964, p. 88.
14. G. R. Chanani, S. D. Antolovich, and W. W. Gerberich: "Fatigue Crack Propagation in Metastable Austenitic Steels", Met. Trans., Vol. 3, No. 10, 1972, pp. 2661-2672.

TABLE I NOMINAL COMPOSITION AND HEAT TREATMENT OF RENÉ 80

		<u>Weight % of Element</u>										
		<u>Al</u>	<u>Ti</u>	<u>Cr</u>	<u>Mo</u>	<u>W</u>	<u>C</u>	<u>Co</u>	<u>B</u>	<u>Zr</u>	<u>Ni</u>	<u>NV.*</u> <u>3</u>
<u>Min.</u>		2.80	4.80	13.7	3.70	3.70	0.15	9.0	0.010	0.02	Bal	2.32
**		(3.00)	(4.87)	(13.80)	(4.06)	(3.90)	(0.15)	(9.60)	(0.014)	(0.02)		(2.27)
<u>Max.</u>		3.20	5.20	14.3	4.30	4.30	0.19	10.0	0.020	0.04		

*Average electron vacancy number. This number must be kept less than 2.50 to prevent the appearance of sigma phase in the temperature regime of 1200-1700°F. Sigma phase formation is stress enhanced and leads to a loss of rupture strength and ductility.

**Composition of specimens supplied by MISCO Vendor Analysis. Other elements are:

Mn: <0.10
 Si: <0.10
 P: <0.10
 S: <0.00 22
 Cb: <0.10
 Ta: <0.10
 Cu: <0.10
 V: <0.10
 Hf: <0.10
 Mg: <0.10

Heat Treatment

- a) 2 hrs. @ 2200°F and He quench (solutinize)
- b) 4 hrs. @ 2000°F and He quench (age)
- c) 4 hrs. @ 1925 - FC to 1200°F in 20 min. (coating cycle)
- d) 16 hrs. @ 1400°F - AC to RT (final age)

This treatment develops a duplex structure.

TABLE II. COMPOSITION AND HEAT TREATMENT OF RENÉ 77 USED IN THIS STUDY

Weight % Of Element

<u>Al</u>	<u>Ti</u>	<u>Cr</u>	<u>Mo</u>	<u>W</u>	<u>C</u>	<u>Co</u>	<u>B</u>	<u>Zr</u>	<u>Ni</u>
4.55	3.73	14.58	5.12	-	0.152	18.78	0.021	<0.02	Bal

Heat Treatment

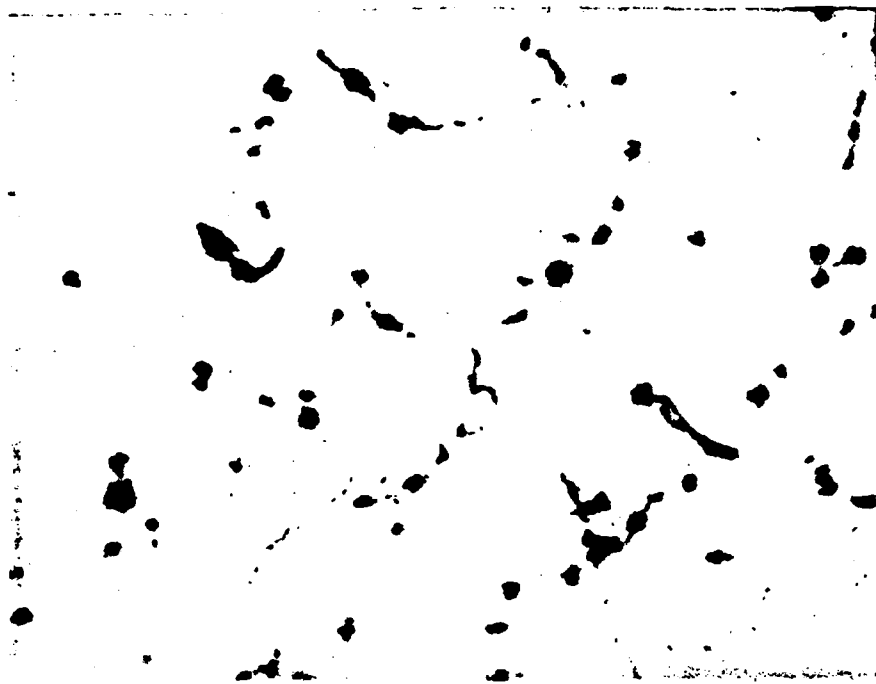
- 1) 4 Hrs. @ 2135 F - AC
- 2) 4 Hrs. @ 1975 F - AC
- 3) 24 Hrs. @ 1550 F - AC
- 4) 16 Hrs. @ 1400 F - AC

This heat treatment develops a duplex γ' precipitate morphology.

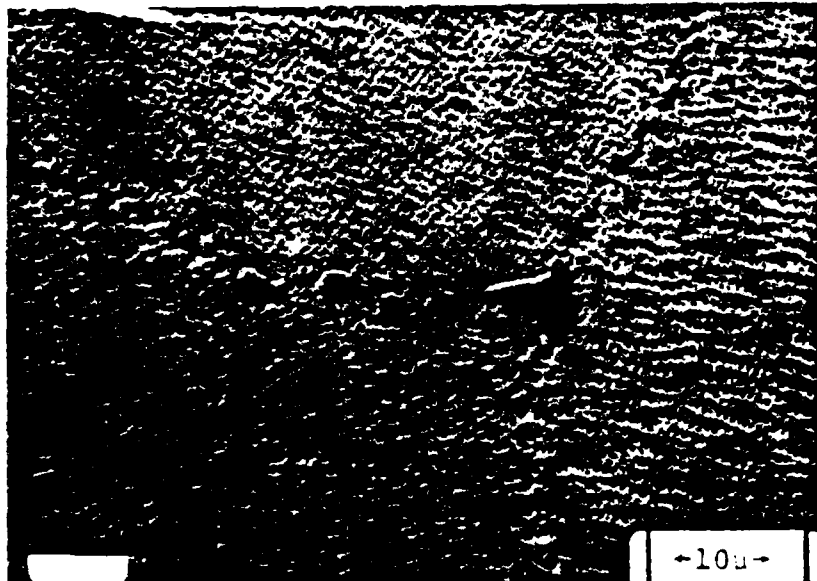
Mn	< 0.05
S	0.002
Si	< 0.10
Cu	< 0.02
Fe	0.37

TABLE III. SUMMARY OF RESEARCH PERSONNEL ASSOCIATED WITH PROJECT

<u>Name</u>	<u>Title and Dates of Project Participation</u>	<u>Topic or Area of Responsibility</u>	<u>Present Status</u>
1. Stephen D. Antolovich	Principal Investigator Jan. 1, 1976-Dec. 31, 1979	Over-all project responsibility.	Professor of Materials Science, University of Cincinnati
2. S. Liu	Research Associate Dec. 1, 1978-Dec. 31, 1979	Electron microscopy studies.	Presently employed by Special Metals
3. B. Roursier	Research Engineer Apr. 1, 1979-Dec. 31, 1979	General assistance with testing and metallography.	Presently Research Engineer assisting on other projects.
4. A. Prakash	Graduate Research Assistant Sept. 9, 1979 - Dec. 31, 1979	General assistance with testing metallography and laboratory development.	Pursuing Ph.D. on AFOSR 80-0065.
5. Paul Domas	Graduate Research Assistant pursuing Ph.D. Jan. 1, 1976-Dec. 31, 1979	Elevated temperature notch fatigue life predictions including hold time effects.	Ph.D. expected Aug. 1980. Draft complete.
6. R. Baur	Graduate Research Assistant pursuing M.S. Jan. 1, 1976-Dec. 31, 1979	Hold time effects in smooth bar LCF.	MS expected Aug. 1980. Draft complete.
7. A. Aizaz	Graduate Research Assistant pursuing Ph.D. Jan. 1, 1976-June 1978	The relationship between LCF and FCP at high temperatures in René 80.	Presently employed by Cabot Corp.
8. E. Rosa	Graduate Research Assistant pursuing M.S. Sept. 27, 1976 - Sept. 30, 1978	Metallography of René 77 LCF specimens.	M.S. Completed, Aug. 1978.
9. J. L. Strudel 10. A. Pineau	Group Leaders at Centre des Matériaux, France. Jan. - June 30, 1976	Discussion of results.	-----
11. J. Ritter	Senior Student completing senior thesis. Sept. 1978-June 1979	Hold-time effects in smooth bar LCF.	Senior Thesis completed, June 1979.
12. J. Telesman	Senior Student completing senior thesis. Sept. 1978-June 1979	Hold-time effects in smooth bar LCF.	Senior Thesis completed, June 1979.



(a)

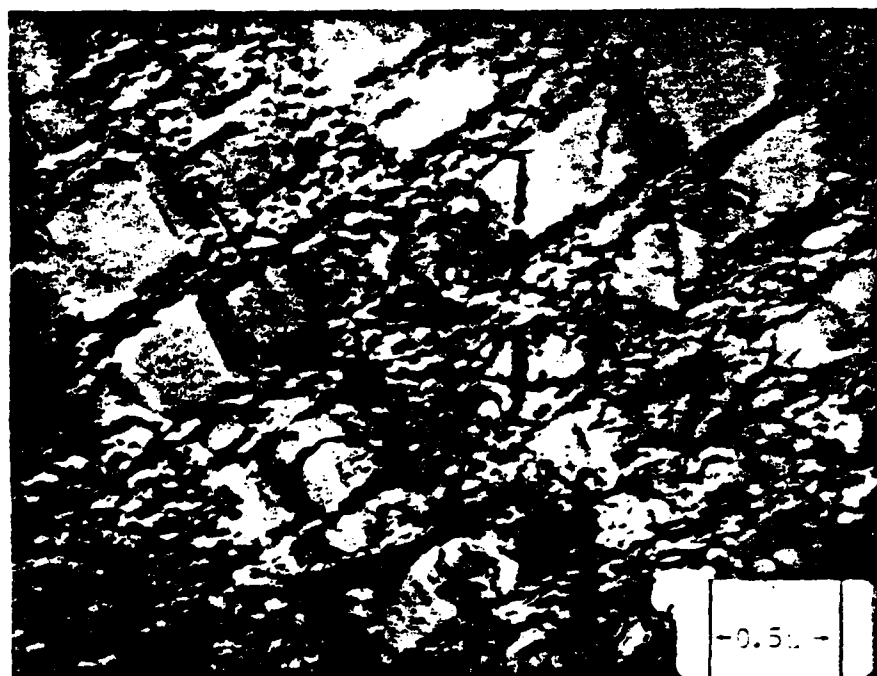


(b)

Fig. 1 Microstructure of as-heat treated René 80. In (a) the irregular nature of the boundaries and the carbides are revealed using a Murakami's etch. In (b) a SEM micrograph shows the cuboidal matrix: γ' , as well as the discrete carbides and γ' in the boundaries.



(a)



(b)

Fig. 2 Morphology of ω' and dislocation substructure of as-heat treated specimens. In (a) the dark field image of the ω' was formed using a $[010]$ superlattice reflection, while in (b) an $[020]$ reflection was used to form the bright field image. Note the duplex ω' morphology in (a) and the very low dislocation density in (b).

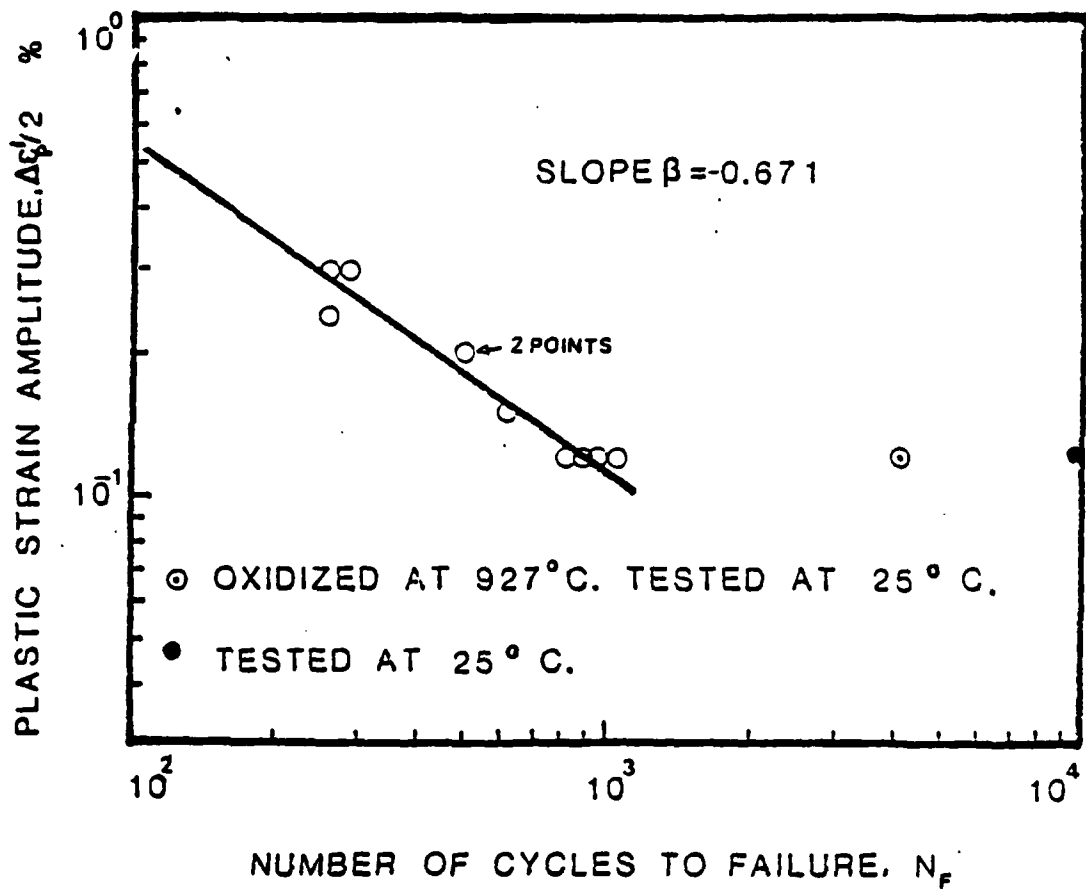


Figure 3. LCF behavior of René 77 at 25°C and 927°C. The oxidized specimen was re-heat-treated before being tested at room temperature.

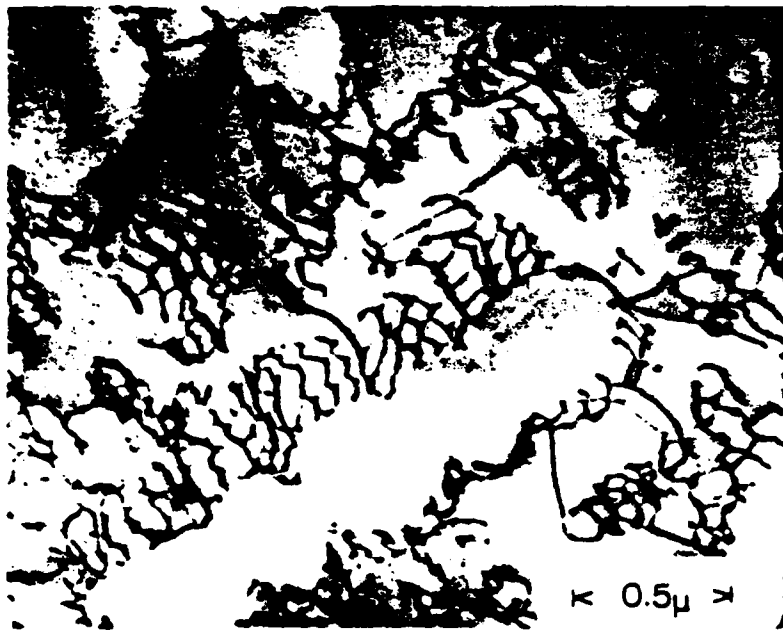


Fig. 4. Interfacial hexagonal networks in a specimen cycled to failure, $N_f = 1090$ cycles. René 77.

$$\Delta \epsilon_p / 2 = 0.121$$

$$T = 927^\circ\text{C}$$

THIS PAGE IS BEST QUALITY PRACTICABLE
FROM COPY

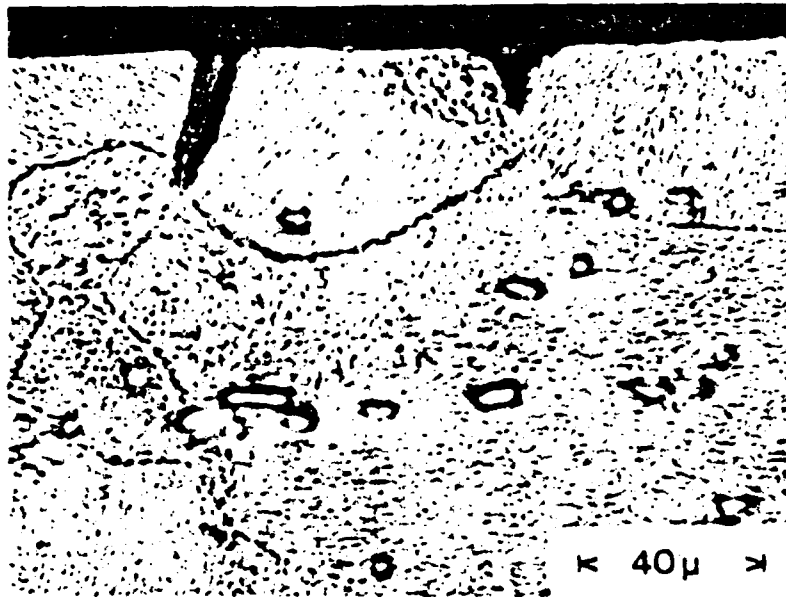


Fig. 5. Oxidized grain boundaries and grain boundary cracking observed in a low strain HTLCF specimen. René 77.

$$\Delta \epsilon_p^c / 2 = 0.12\% \quad N_f = 320 \text{ cycles}$$

$$T = 927^\circ\text{C}$$

THIS PAGE IS BEST QUALITY PRACTICABLE
FROM COPY FURNISHED TO DDC

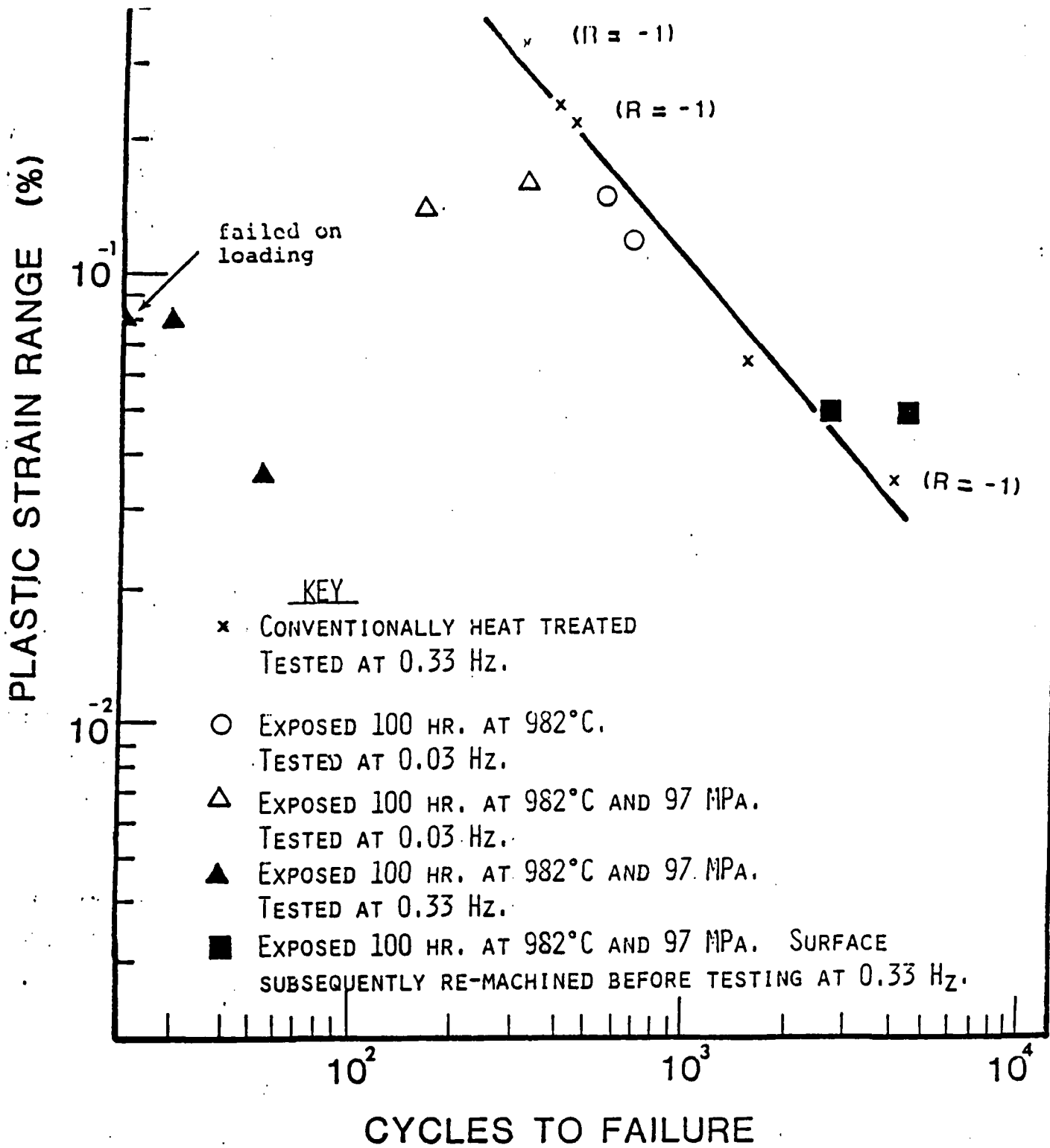


Figure 6. Coffin Manson plot of LCF data for René 80 at 871°C. All testing done at R = 0.05 except as noted.



(a) $g = [1\bar{1}1]$

$\leftarrow 1\mu \rightarrow$



(b) $g = [1\bar{1}\bar{1}]$

Fig. 7. Precipitate/dislocation structure of specimen LSA3 which was fatigued at $0.03H_{0.2}$. Life 162 cycles, plastic strain amplitude 0.068% . Note that each reflection is illuminating what are apparently edge dislocations. Figure 7(d) was taken using multiple reflections and all dislocations are illuminated.

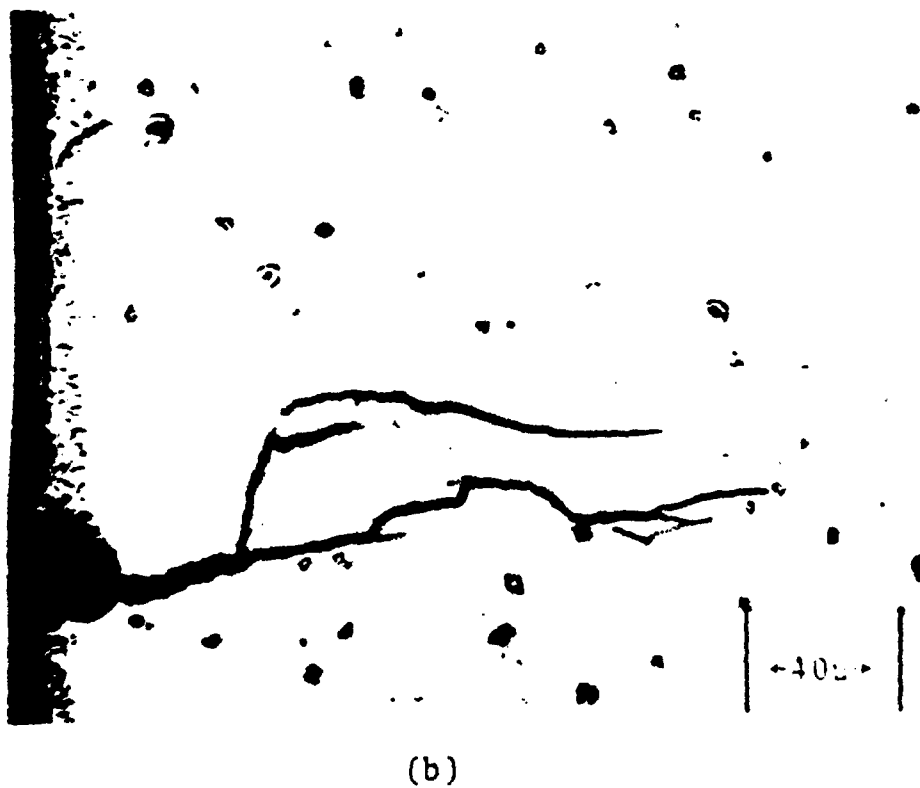


(c) $g = [002]$

$\leftarrow lu \rightarrow$

(d) (multibeam)

Fig. 7.



THIS PAGE IS BEST QUALITY PRACTICABLE
FROM COPY FURNISHED TO DDC

Fig. 8. Microcrack formation in (a) thermally exposed and (b) thermally plus stress exposed specimens. Both specimens were tested at $0.05 H_2$. The boundaries of the thermally exposed specimens could generally tolerate more oxidation before forming microcracks.

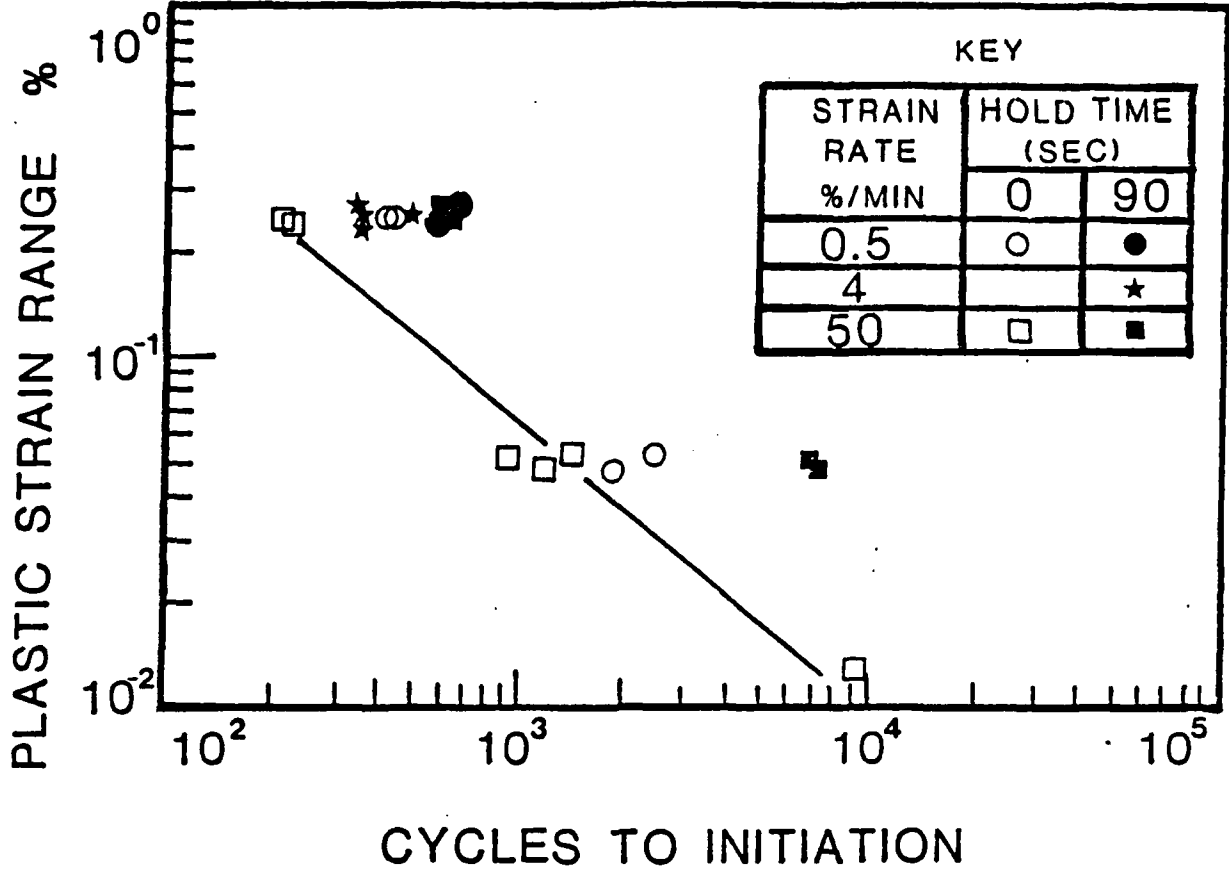


Fig. 9. LCF behavior of René 80 at 871°C (1600°F).

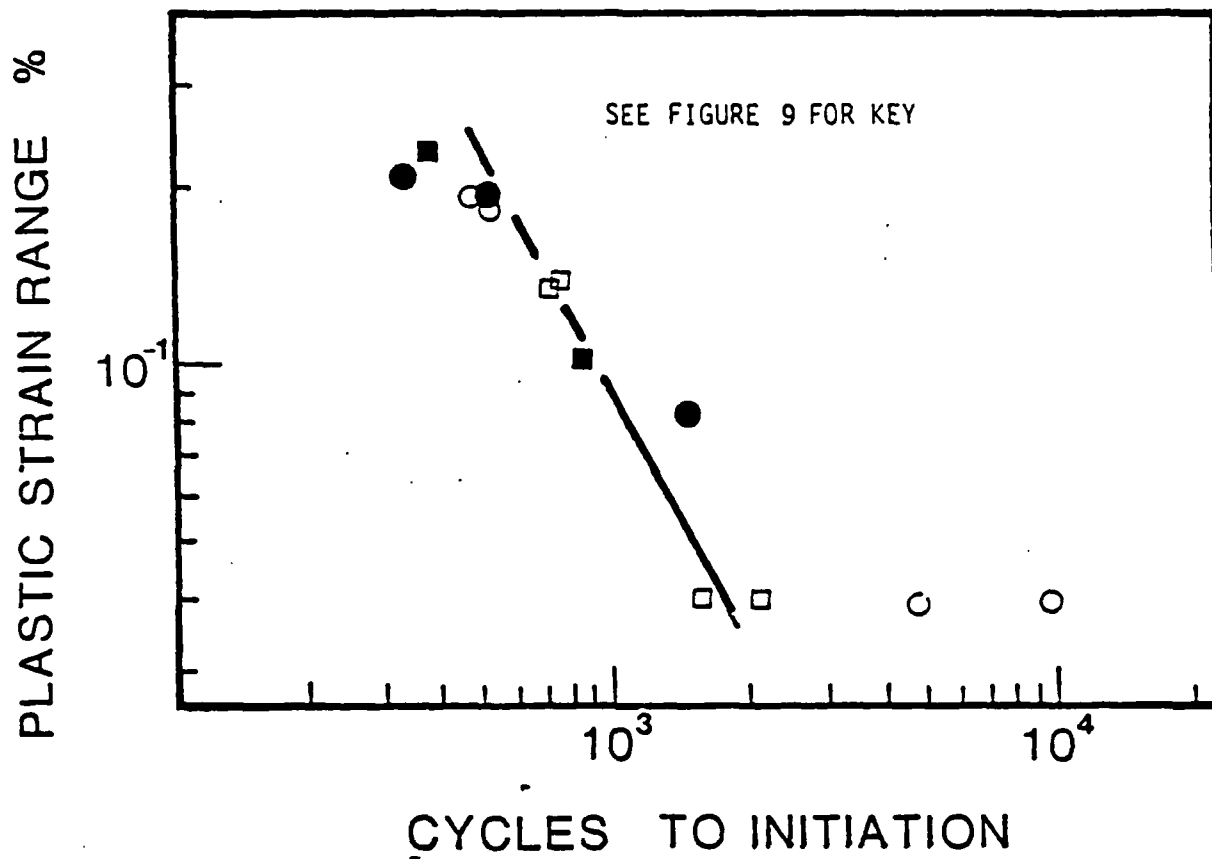


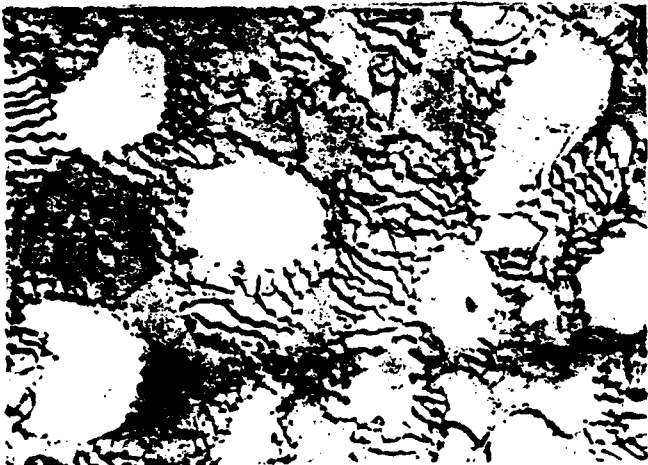
Fig. 10. LCF behavior of René 80 at 982°C (1800°F).



(a)



(d)



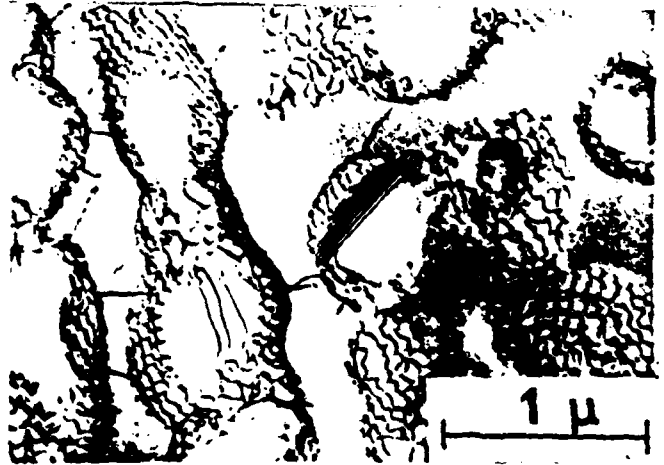
(b)



(e)



(c)



(f)

THIS PAGE IS BEST QUALITY PRACTICABLE
FROM COPY FURNISHED TO DDC

Fig. 11. Representative structural changes for specimens tested at 1600°F (a-c) and 1800°F (d-f). Compare to the as-heat treated structure shown in Fig. 2b. Specific test conditions are as follows:

(a) $\Delta\epsilon_p = 0.25\%$, $\dot{\epsilon} = 50/\text{min}$ $N_f = 312$

(b) $\Delta\epsilon_p = 0.25\%$, $\dot{\epsilon} = 0.5/\text{min}$ $N_f = 732$

(c) $\Delta\epsilon_p = 0.25\%$, $\dot{\epsilon} = 0.5/\text{min} + 90\text{s hold}$
 $N_f = 929$

(d) $\Delta\epsilon_p = 0.04\%$, $\dot{\epsilon} = 53/\text{min}$ $N_f = 2511$

(e) $\Delta\epsilon_p = 0.18\%$, $\dot{\epsilon} = 0.5/\text{min}$ $N_f = 877$

(f) $\Delta\epsilon_p = 0.196\%$, $\dot{\epsilon} = 0.5/\text{min} + 90\text{s hold}$
 $N_f = 573$

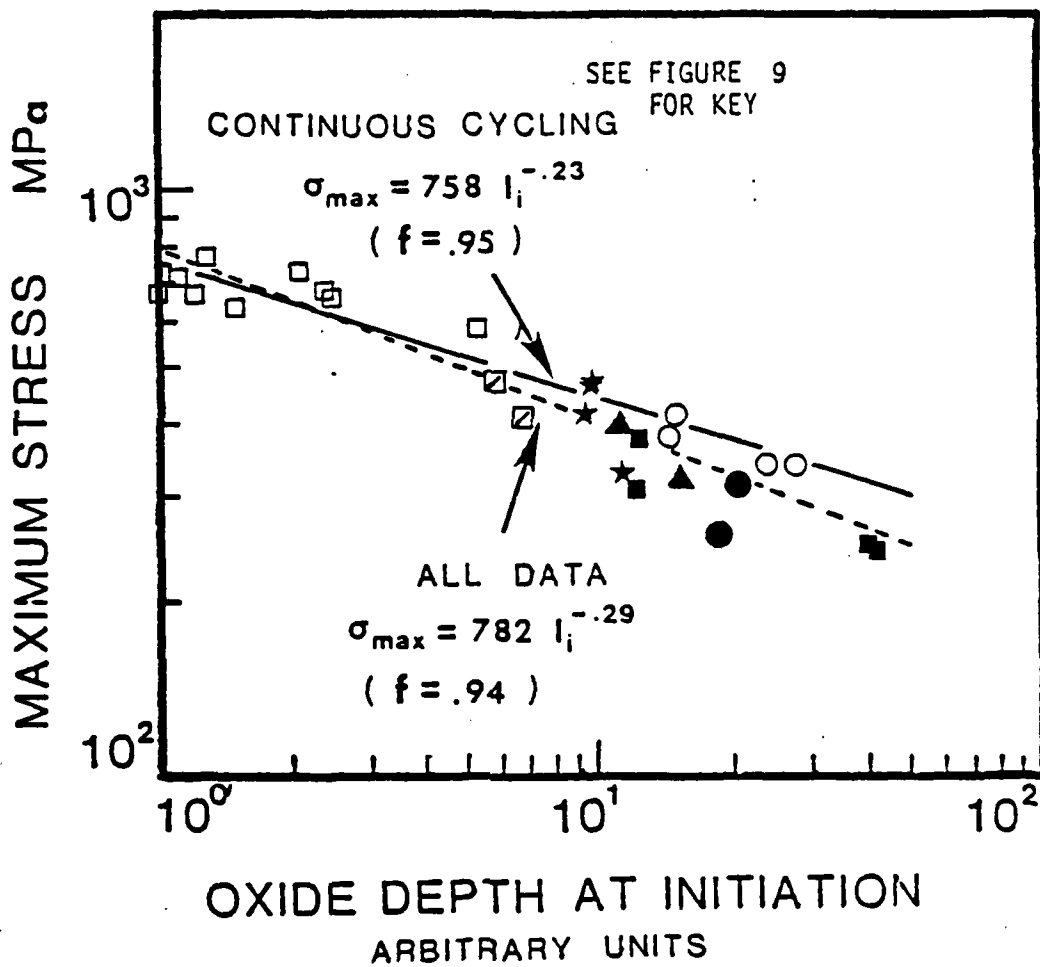


Fig. 12. Maximum stress at initiation vs. oxide spike depth for specimens tested at 871°C.

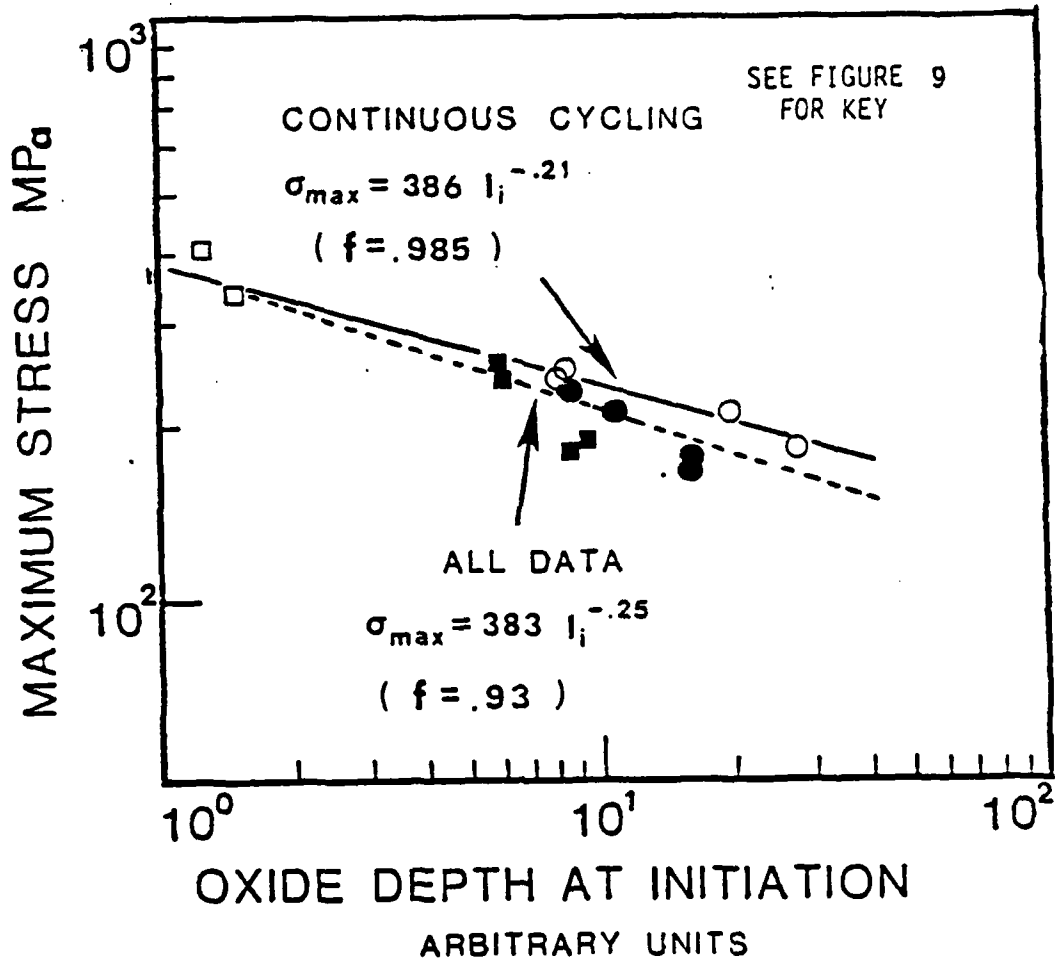


Fig. 13. Stress at initiation vs. oxide spike depth for specimens tested at 871°C (1600°F).

Fig. 17 Cumulative Plastic Volume Change, Density (Graph)

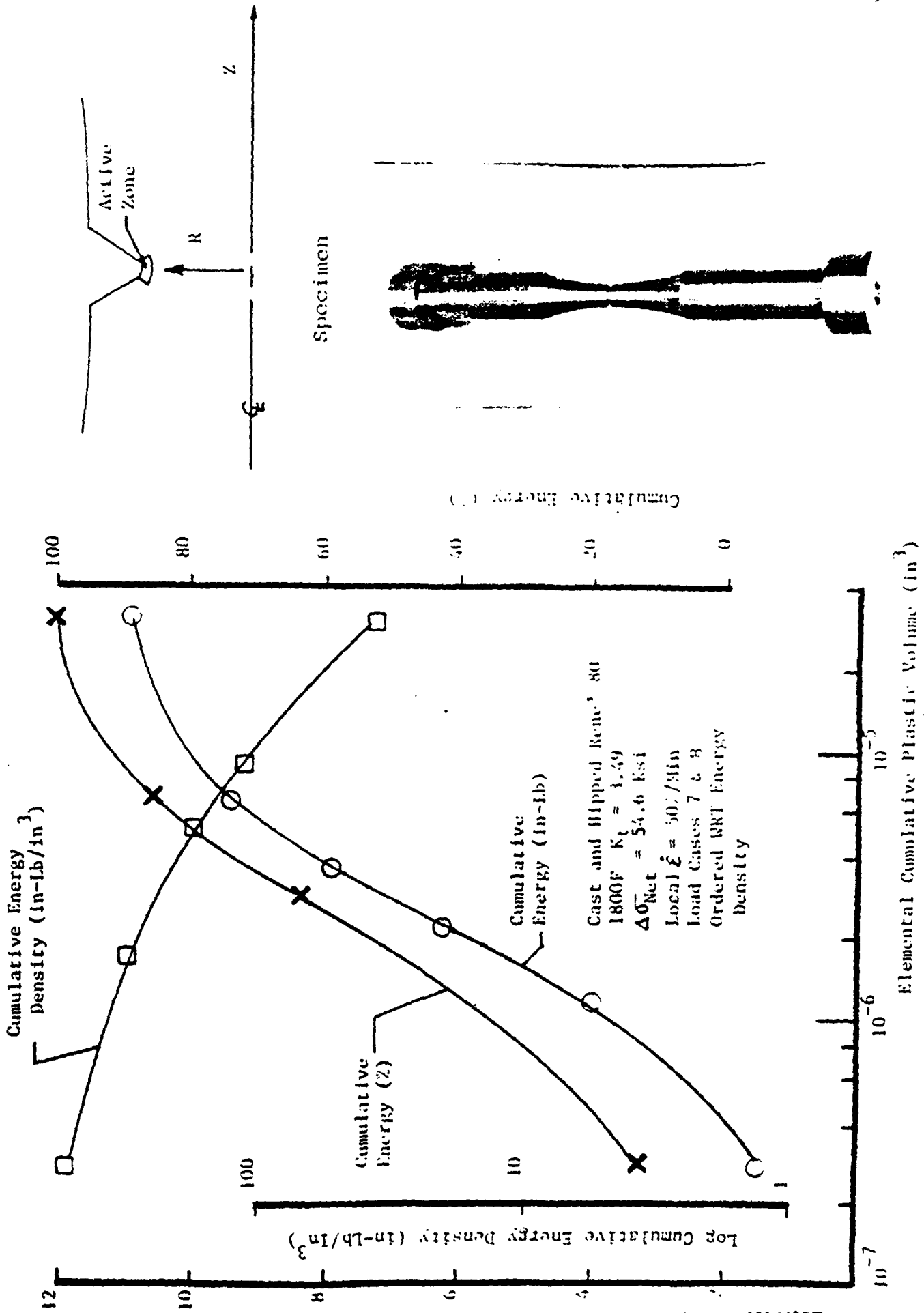


Fig. 15. Comparison of Notch Life Prediction and Test Results

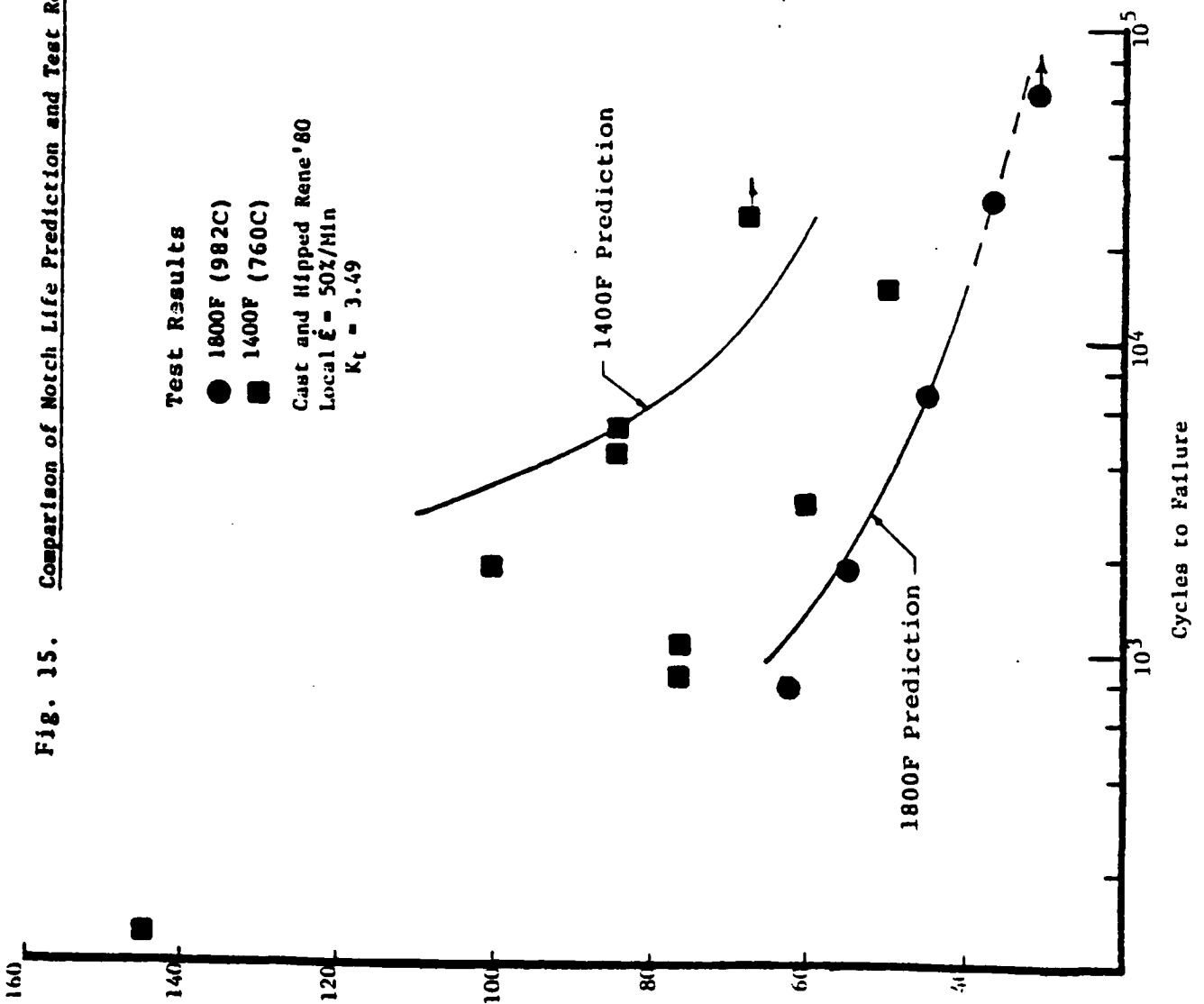


Figure 16: NOTCH LOW CYCLE FATIGUE TEST RESULTS
 982C (1800F), $K_T = 3.49$

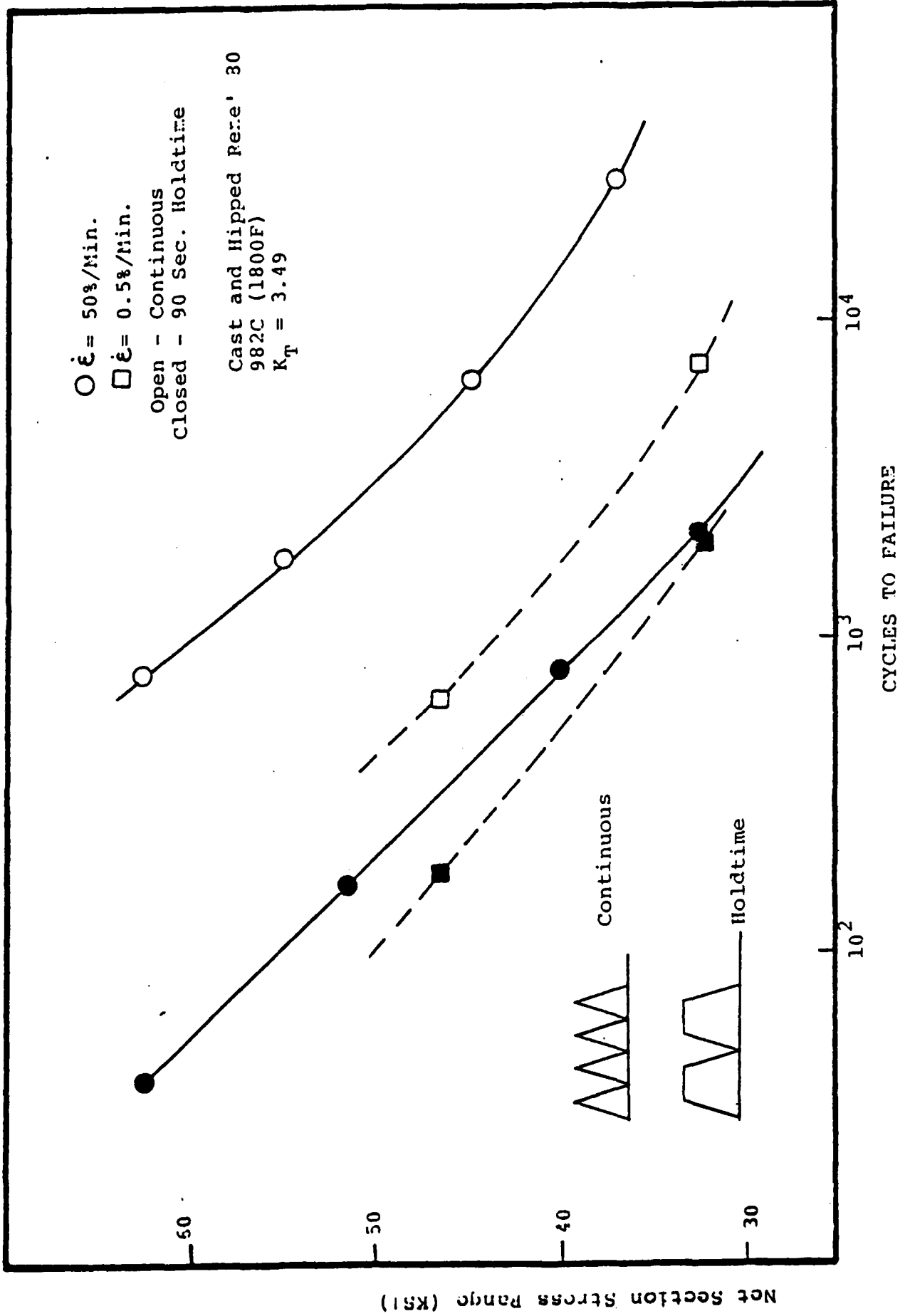


Figure 17: NOTCH LOW CYCLE FATIGUE TEST RESULTS
 982C (1900F), $K_T = 2.22$

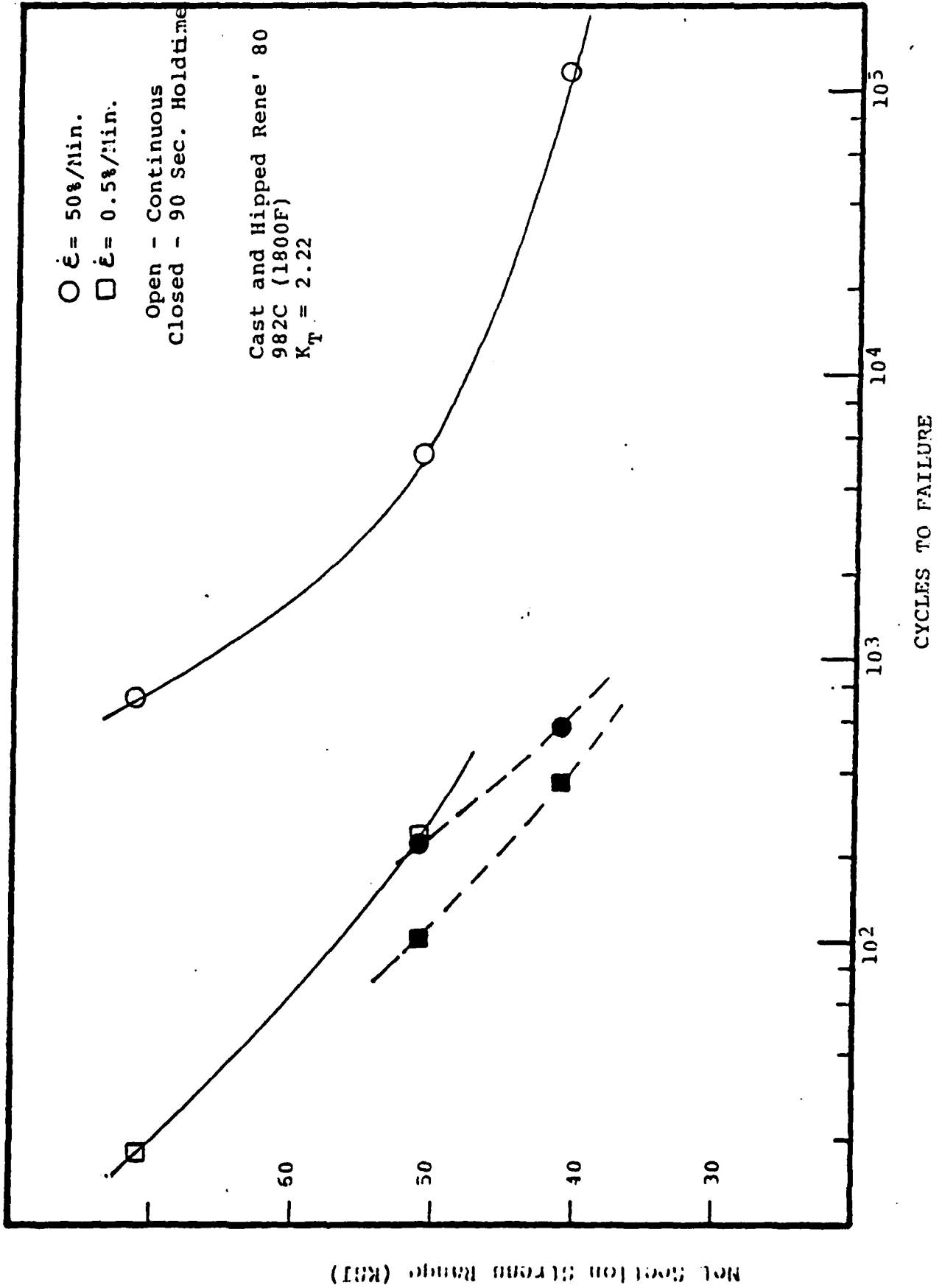
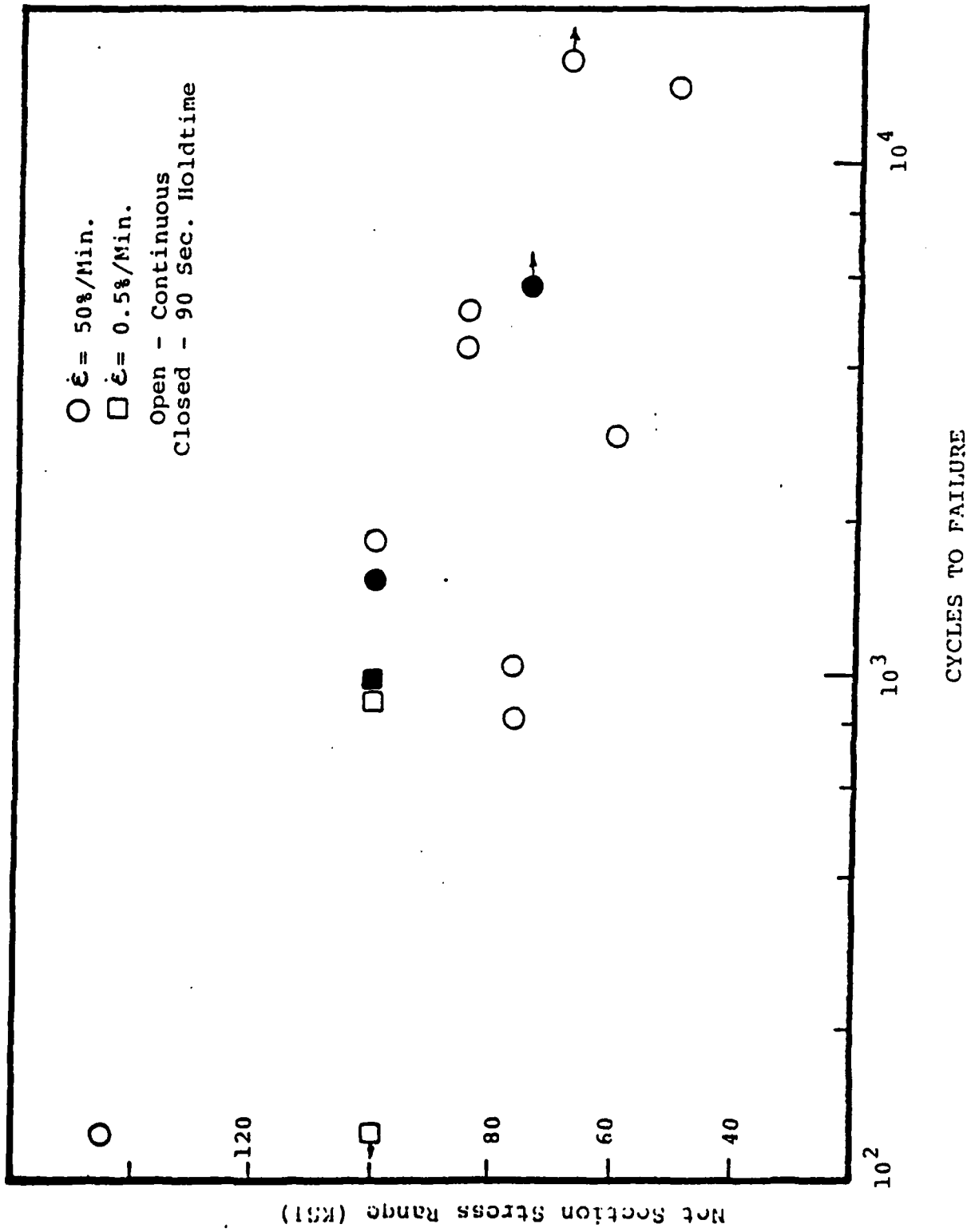


Figure 18: NOTCH LOW CYCLE FATIGUE TEST RESULTS
 760C (1400F), $K_T = 3.49$



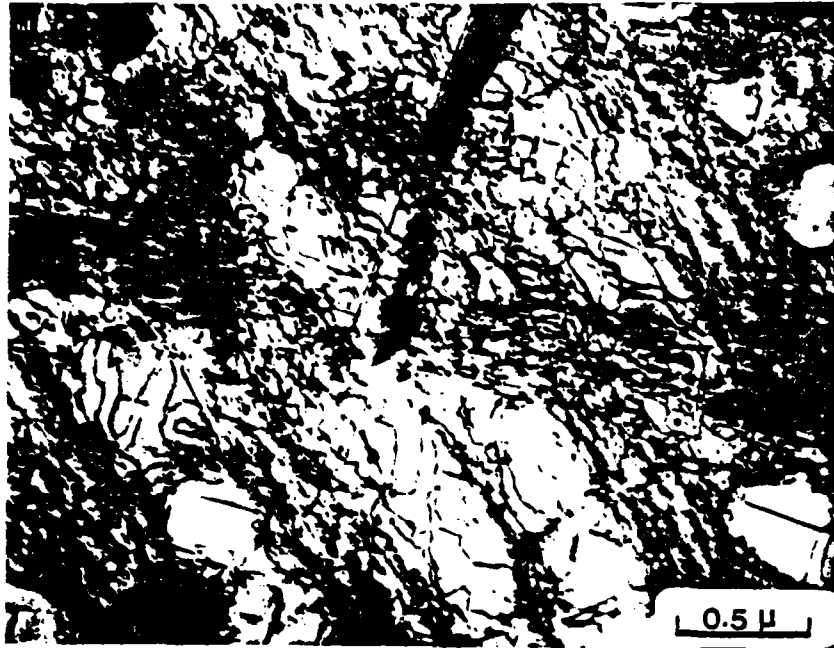


Fig. 19. Deformation substructure of René 80 LCF specimen tested at 1400°F (760°C). Note the small precipitates have not dissolved as evidenced by the strain contrast between the large cuboidal precipitates. Note also the planar slip band and the linear dislocation segments that have penetrated the large particles.

$\nabla\epsilon_p = 0.075\%$. $N_f = 535$ cycles Specimen 14LV22.

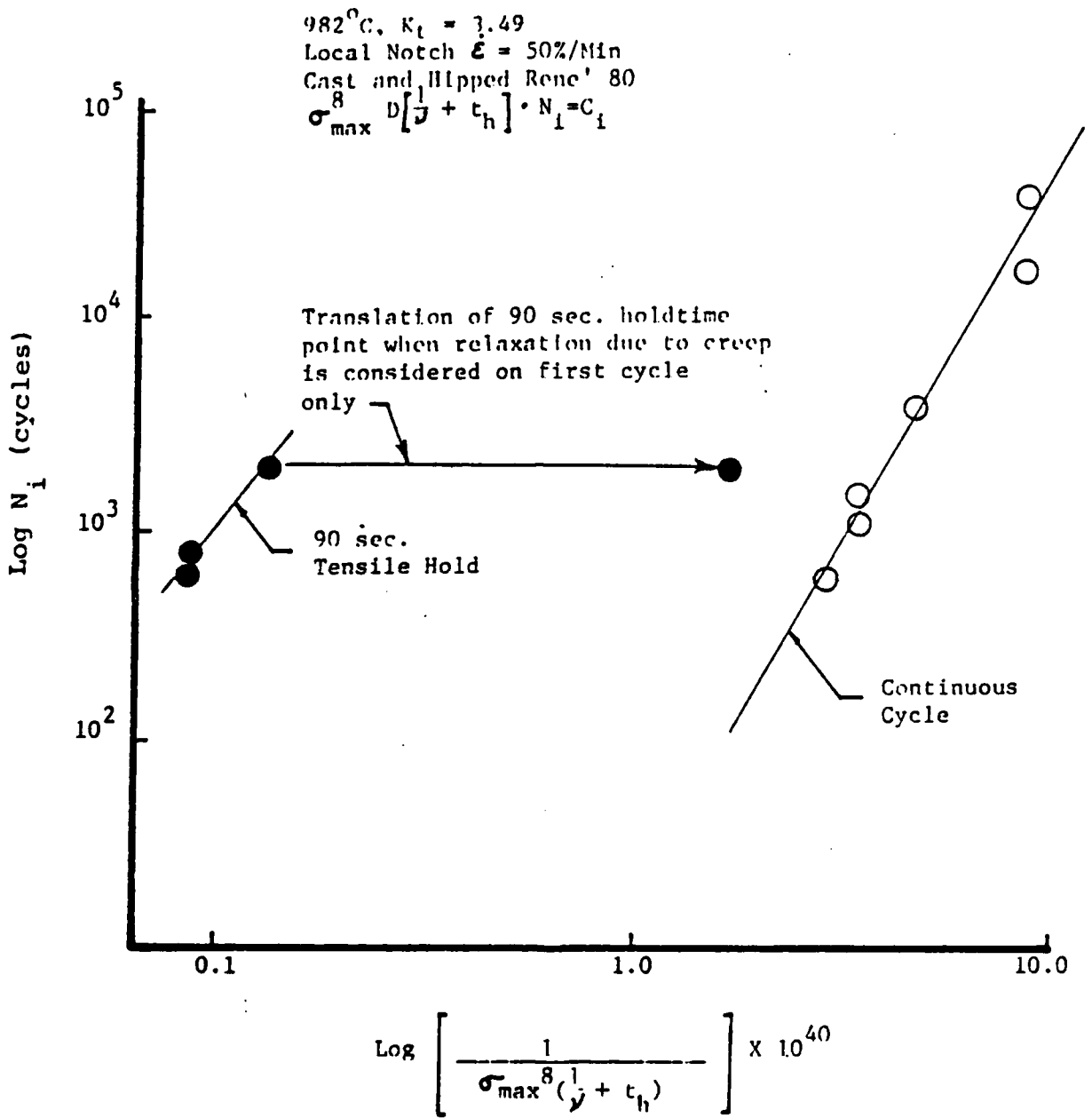


Fig. 20: Correlation of Notched Bar Results with Mechanistic Model

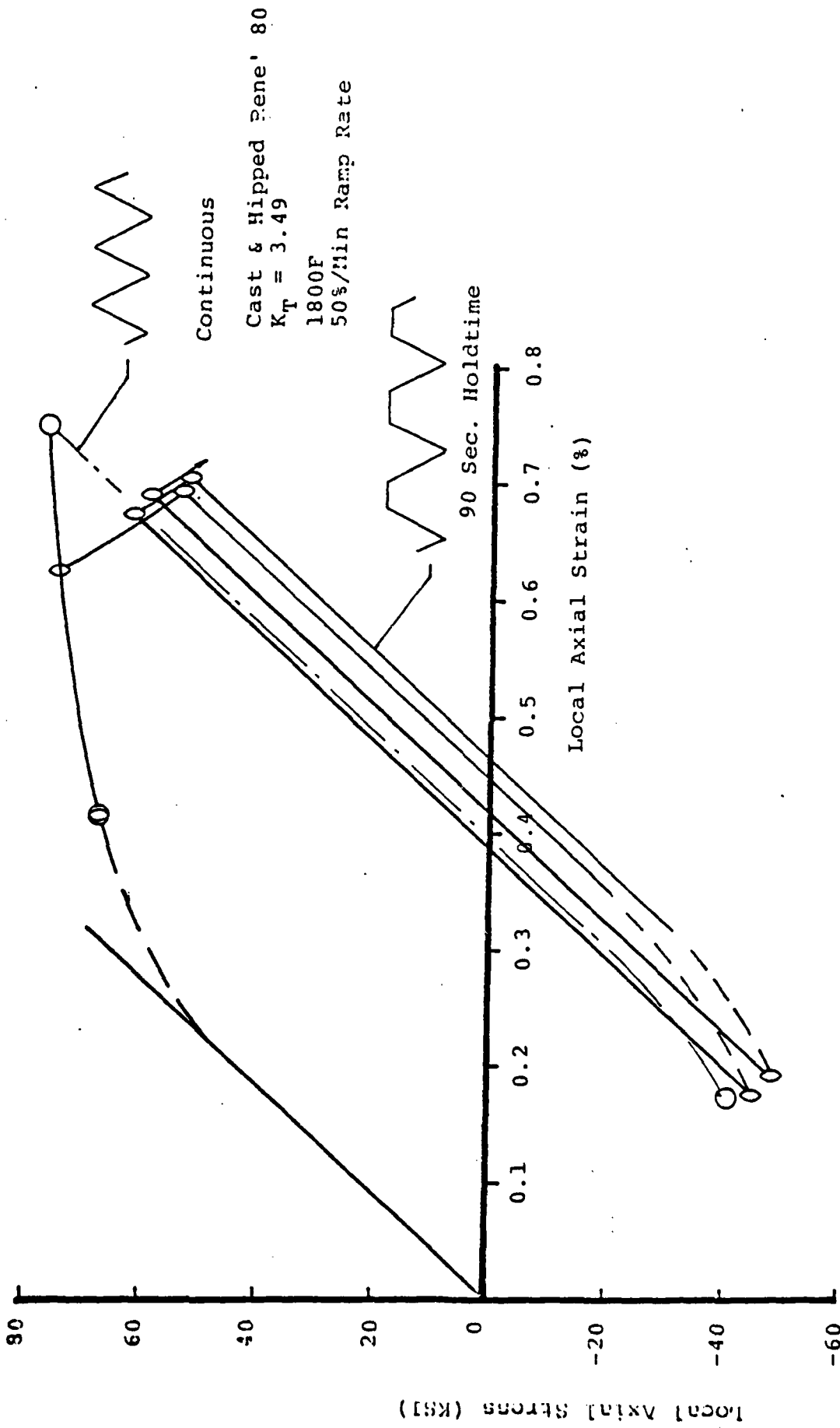


Fig. 21: PREDICTED NOTCH ROOT STRESS-STRAIN RESPONSE